Thermal Conductivity of Polymeric Aerogels at Vacuum for Cryogenic Insulation Applications

J. A. Demko[1]*, G. Churu[1], R. Ehresman[1], T. Fiorenzi[1], A. Libiez[1], D. Dugan[1], H. McGuire[1], A. Moore[1], W. Johnson[2], S. Malakooti[2], and S. L. Vivod[2]

[1] Mechanical Engineering Department, LeTourneau University, Longview, TX USA
[2] Materials and Structures Division, NASA Glenn Research Center, Cleveland, OH, USA

*E-mail: jonathandemko@letu.edu

Abstract. Effective management of the heat transfer into cryogenic piping, storage reservoirs used to contain liquefied gases such as nitrogen, hydrogen, and helium, or other cryogenic applications is accomplished with low thermal conductivity insulation systems. Aerogels are known for their low density, high mesoporosity, high surface areas, low thermal conductivity and high acoustic impedance. This study focuses on polymeric aerogels that can be mass produced as large monoliths while maintaining the low thermal conductivity over a wide temperature range. To measure the thermal conductivity, a NASA Cryostat-400 flat plate boiloff calorimeter was used to measure the thermal conductivity of these materials at residual gas pressures ranging from high vacuum, soft vacuum, and atmospheric pressure. The calorimeter uses boiloff of liquid nitrogen to measure the heat transfer through the insulation sample. Measurements of the thermal conductivity will be between a cold boundary temperature maintained by the liquid nitrogen (80 K) and a hot boundary at room temperature (290 K). A pressure control system will be used to maintain pressure in the cryostat at different levels using nitrogen as the residual gas. For better understanding of the heat transfer measurement, a numerical model of the system was developed in Python.

1. Aerogels

Aerogels are traditionally produced by removing the liquid from gels using supercritical fluid extraction. The process results in a highly porous, low-density material with a very high surface area. The gels can be made from materials such as silica, polymers, and metals. The aerogel type of material has low thermal conductivity. The size of the aerogel samples that can be made is limited by the size of the autoclave used.

Polymer aerogels are created from a polymer-based gel with many of the traits of more common silica aerogels. Figure 1 includes a scanning electron microscope images of (a) a templated silica aerogel and (b) a polymer aerogel [1]. Both materials exhibit similar characteristics. But as seen in the images, the silica-based aerogel has a different structure than the polymer aerogel. Figure 2 is an example of the machinability of the polymer aerogel. A cylinder as seen in the lower specimen, has been machined on a lathe to produce the pipe structure that is on top. The aerogel of this study uses a low vapor pressure fluid during the final processing stage and can be dried in ambient conditions, thus eliminating the need for supercritical drying. Thus,

the resulting materials are robust and can be produced in larger sizes than traditional silica aerogels while maintaining comparable thermal properties.

Since aerogels are porous the thermal conductivity depends on factors including the type of matrix material (silica, polymer, etc), the density (porosity), and the presence of interstitial gases. Common interstitial gases include atmospheric air, nitrogen, or helium. Measurements of the thermal conductivity in a pipe configuration as shown in Figure 2c indicated that for the polymer aerogel tested, the thermal conductivity in the presence of helium at slightly higher than atmospheric was nearly that of the helium alone [2]. The thermal conductivity of organic aerogels in thick disk samples and series of thin disks were measured in [3]. In addition, the electrical breakdown characterization was conducted at 77 K and room temperature. The purpose of this study is to measure the dependence of thermal conductivity on the pressure in the insulation from high vacuum ($\sim 1\ \mu bar$) to atmospheric pressure. Gaseous nitrogen is the background gas.

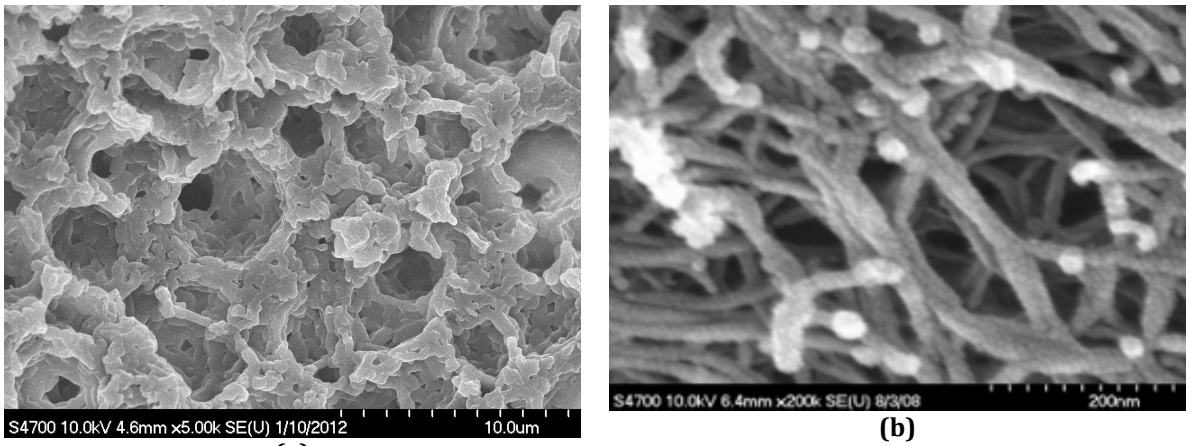

(a) **(b)**

Figure 1. Scanning electron microscope (a) silica aerogel and (b) polymer aerogel, showing the characteristic highly porous morphology and large surface of aerogel materials

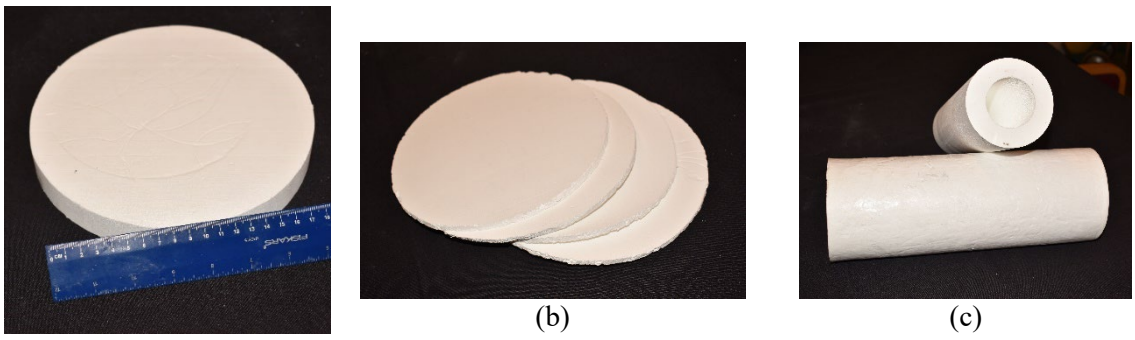

(a) (b) (c)

Figure 2. Polymer aerogel (a) thick disk, (b) series of thin disks, and (c) cylinder as cast and after machining into a hollow cylinder.

2. Experimental apparatus and procedure

The thermal conductivity can be determined using one-dimensional heat conduction in a plane according to the equation:

$$k = \frac{\dot{Q} \times \Delta L_{sample}}{\Delta T \times A_{sample}} \quad (1)$$

Where k is the thermal conductivity in W/m·K, $\dot{Q}$ is the measured heat transfer, ΔL_{sample} is the thickness of the sample in meters, ΔT is the measured temperature between the warm boundary and the cold boundary, and A_{sample} is the heat transfer area of the sample in m^2. The heat transfer is determined using a NASA Cryostat-400 [4,5,6]

2.1 NASA Cryostat 400

The Cryostat-400 test apparatus is a comparative, flat-plate instrument, with a cryogenic boil-off calorimeter. It was chosen for this effort for the relative simplicity and ease of operation of this apparatus compared to other insulation test cryostats. Another important reason is the suitability for testing rigid, flat disk type materials in pressure environments from vacuum ($\sim$1 μbar) to atmospheric pressure [4].

Evaporation (or boil-off) calorimetry reflects real-world conditions of cryogenic piping and cryostats and it thus provides a straightforward approach for testing low-temperature thermal insulation systems. For representative test conditions in sub-ambient temperature applications, it is worth reiterating that the temperature difference is the driver for heat transmission. Thermal conductivity data reported as a function of temperature are good to have but can be misleading when applied to field performance. Figure 3 shows a CAD model, showing a cut-away of the Cryostat 400 instrument, a CAD model of the cold mass, and the Cryostat 400 set up in the laboratory at LeTourneau University. Specific details of the Cryostat-400 are given in a number of publications [5,6].

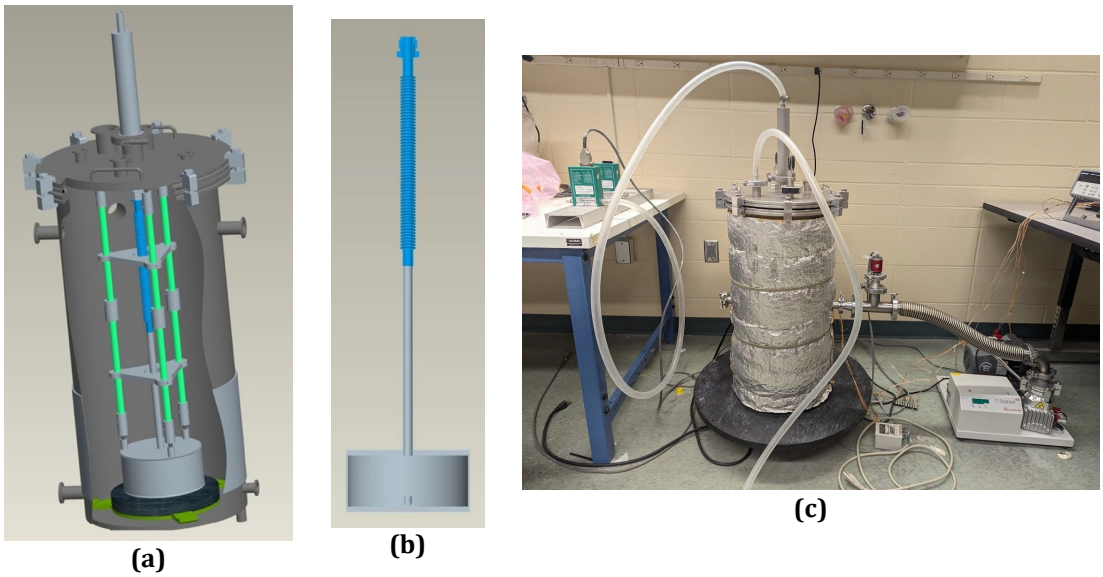

(a) **(b)** **(c)**

Figure 3. (a) CAD model showing a cut-away of the Cryostat 400 instrument, (b) CAD model of the cold mass, and (c) the Cryostat 400 in the laboratory at LeTourneau University.

Type K thermocouples are used to measure the cold boundary temperature (CBT) and warm boundary temperatures (WBT) and are located as shown in Figure 4. As shown in the figure there

are three thermocouples on the cold mass with T_1 in the center, T_2 and T_3 located approximately half way between the center and the outer radius of the liquid nitrogen-filled vessel. On the warm boundary a similar arrangement of thermocouples is used with T_4 on the center, T_5, T_6 at similar radial positions. Two additional thermocouples, T_7 and T_8 are located at the center of the cold and warm boundaries of the sample.

The mass flow is measured by a MKS Model M10MB mass flow meter calibrated for gaseous nitrogen flow. The temperatures and voltage outputs from the mass flow meters are read using a Keysight 34970A data acquisition / switch unit. Data is sampled every 30 seconds for the duration of an experiment run which typically lasts over 10 hours.

Two methods are used to determine the CBT and WBT from the measured temperatures and are used to determine the thermal conductivity. The center temperatures T_1 for the CBT and T_4 for the WBT is the first method. But since there is a slight variation over the different tempeatures, an average of T_1, T_2, and T_3 is calculated for the average CBT and an average of T_4, T_5, and T_6 are calculated for the average WBT.

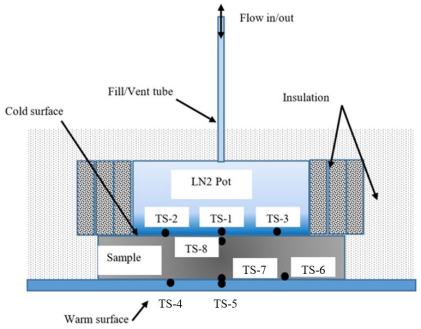

Figure 4. Location of thermocouples on Cryostat-400 cold mass.

2.2 Vacuum pressure control

At the present time, only the atmospheric and high vacuum configurations shown in Figure 5 (a) and (b) are operational. The necessary components for controlling the vacuum pressure are currently being installed. For the atmospheric pressure measurement, the cryostat is open to atmosphere and a very slight purge flow of nitrogen gas is supplied to the chamber. This is to prevent any back flow of humid atmospheric air into the chamber which would condense and freeze moisture in the sample. For the high vacuum test, all ports are closed except that there is a safety relief on the chamber. An Edwards T-85 turbo vacuum pump system is used to reduce the pressure in the chamber. Pressure is measured using an Edwards D1G1021150 Tungsten/Rhenium filament Pirani gauge with a range from atmosphere to 1 μbar, that is located close to the cryostat on the pump out line.

The pressure control system, which has not yet been implemented, is shown schematically in Figure 5(c). It consists of the Edwards T-85 vacuum pump, an MKS-946 vacuum controller that operates a MKS O248D-1000SV solenoid valve. The valve will supply gaseous nitrogen as needed to maintain the desired pressure level in the cryostat.

A cellular glasss test specimen, shown in Figure 6, that was used in a previous study [6] was chosen for a control and used to calibrate the current set-up. The aerogel test specimen was

machined to the following nominal dimensions: 203-mm diameter by 25.4-mm thickness by the NASA KSC Cryo Test Lab and supplied to LeTourneau University for testing.

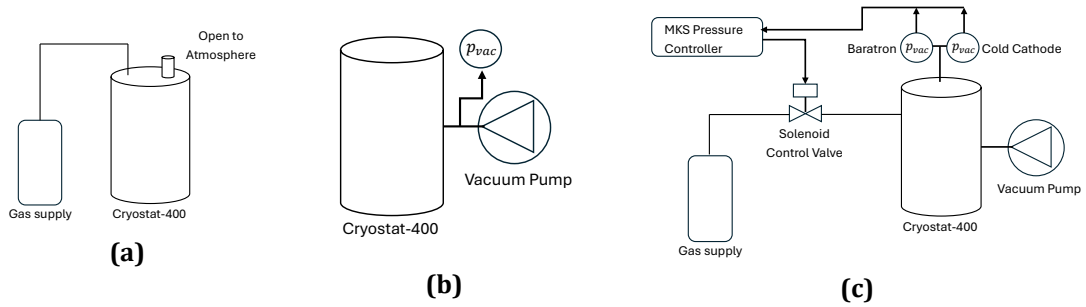

Figure 5. Test arrangements for different pressure conditions. (a) atmospheric pressure, (b) high vacuum, and (c) variable pressure.

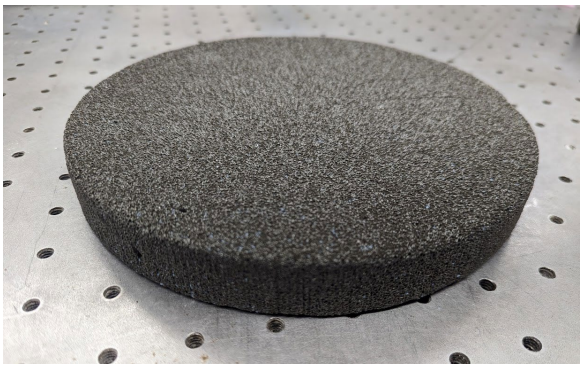

Figure 6. Typical test specimen of a cellular glass material

3. Results

Test results so far consist of measurements of the cellular glass sample at atmosphere and at high vacuum. Figure 7 (a) and (b) shows measured temperatures and nitrogen boil-off flow for the atmospheric pressure case. In figure 5(a) the temperatures correspond to the locations of TS-1 (101), TS-2 (102), TS-3 (103), TS-5 (105), TS-6 (106), and TS-7 (107) as shown in Figure 4.

The initial cooldown starts at t=0 hours as shown by the rapid drop in temperature. After about 1.5 hours there is an increase in temperatures which happened because the nitrogen pot boiled-off all the liquid. The test procedure is typically run with a number of nitrogen refills until a steady boil-off rate as shown in Figure 7(b) is reached. The only time during this run that the pot ran dry was around 1.5 hours. A zero flow rate at subsequent times is because the flow meter is disconnected since the fill and vent are through the same port. At the start of each fill (or re-fill) the flow is high but settles down quickly to a stable value. The red rectangles represent the times which the temperatures are averaged during the run for determination of the thermal conductivity.

Table 1 lists the average boundary temperatures, taken from the center temperature measurement, and boil-off flow rate for the different times referred to as Run1, Run 2, and Run 3 respectively. These values were used to calculate the thermal conductivity, heat transfer, and heat

flux for the three times. A second row is provided for each run that uses the average temperatures across the cold or warm boundary as discussed previously.

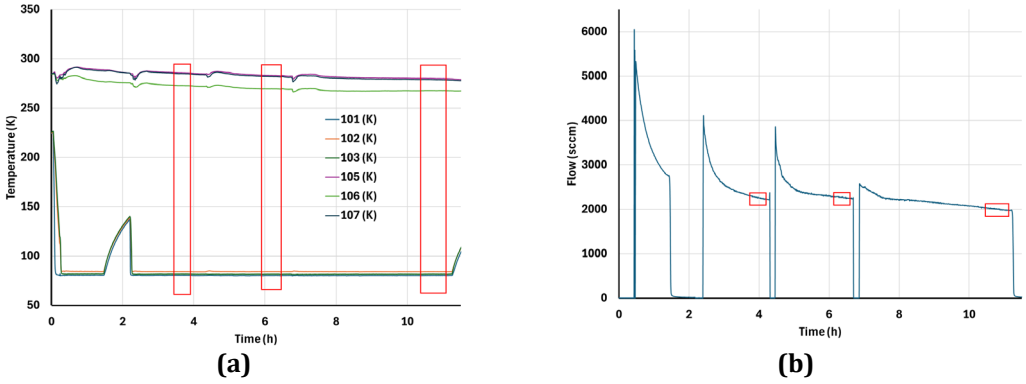

Figure 7. Temperatures and flow measurements for ambient pressure

The first two runs indicate higher flows than the third run resulting in higher conductivity values. Run 3 has been cold for the longest time, approximately 10 hours since the pot went dry the first time, and is the best result.

Table 1. Ambient pressure thermal conductivity results

Test	CBT (K)	WBT (K)	Flow (sccm)	k (W/m-K)	Q (W)	Q/A (W/m^2)
Run 1	80.29	285.2	2261	0.0666	9.358	535.0
T_{Avg}	82.04	280.6	2261	0.0687	9.358	535.0
Run 2	80.23	283.0	2278	0.0678	9.430	539.1
T_{Avg}	82.04	278.2	2278	0.0700	9.430	539.1
Run 3	80.29	280.0	2004.2	0.0606	8.295	474.5
T_{Avg}	82.08	275.5	2004.2	0.0625	8.295	474.5

The high vacuum measured temperature and flow data are in Figure 8 (a) and (b). Figure 8(c) shows the measured vacuum pressures during the measurement. The approach to analyzing the data is the same as for the atmospheric pressure case where the red rectangles represent the times which temperature and flows are averaged to provide the data which determines the thermal conductivity. The averaged boundary temperature and flows are provided in Table 2 along with the reduced thermal conductivity, heat transfer and heat flux data. It is seen that the thermal conductivity has dropped from $k_{atmosphere}$ of between 0.060 to 0.063 W/m·K to k_{vacuum} that ranged from 0.022 to0.024 W/m·K. The atmospheric pressure values correspond to that of previously reported values of between 0.063 to 0.068 W/m·K [5].

The thermal conductivity is expected to decrease when the insulation is evacuated since there would not be any residual gas to transport heat in addition to the aerogel. It is anticipated that the aerogel materials will also exhibit the same decrease. Measurements on a sample of polymeric aerogel demonstrated a large increase in the themal conductivity when helium gas at a slightly elevated pressure was present. The thermal conductivity of the aerogel had limited influence on the overall conductivity [3].

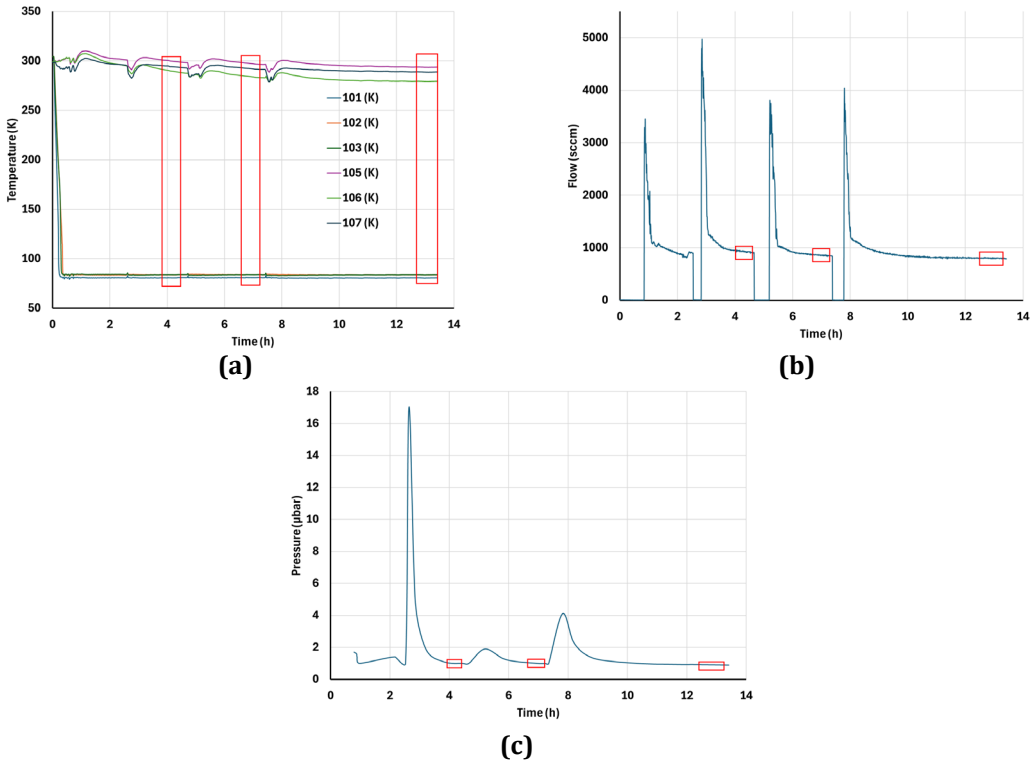

Figure 8. Measured (a) temperatures (b) flow, and (c) vacuum pressure for high vacuum pressure run.

4. Summary and Next Steps

The dependence of the thermal conductivity of porous insulation materials on the insulation pressure has many applications in cryogenic systems. This initial stage of the work was able to conduct thermal conductivity measurement on cellular glass insulation at atmospheric pressure with nitrogen as the background gas, and at a vacuum pressure of 1μbar. The results showed a drop in the thermal conductivity from 0.062 to 0.023 W/m·K.

The next phase of this project is to finish the set-up of the vacuum control equipment and conduct measurement using Cryostat 400, of the thermal conductivity over the range of pressures from 1μbar to atmospheric pressure beginning with the cellular glass material subsequently with polymeric aerogels.

Table 2. High vacuum thermal conductivity results

Test	P_{vac} (μbar)	CBT (K)	WBT (K)	Flow (sccm)	k (W/m-K)	Q (W)	Q/A (W/m^2)
Run 1	1	80.74	299.6	932.5	0.0257	3.860	220.7
T_{Avg}	1	82.68	294.4	932.5	0.0266	3.860	220.7
Run 2	1	80.88	297.2	859.3	0.0240	3.557	203.3
T_{Avg}	1	82.78	291.2	859.3	0.0249	3.557	203.3
Run 3	>1	80.64	293.7	799.0	0.0226	3.307	189.1
T_{Avg}	>1	82.61	287.4	799.0	0.0235	3.307	189.1

Acknowledgments

This research is sponsored by the National Aeronautics and Space Administration (NASA) Glenn Research Center Grant / Cooperative Agreement Number 80NSSC24K1099.
We would like to thank LeTourneau University School of Engineering and Engineering Technology for providing facilities and undergraduate student support for this research.

References

[1] Meador, Mary Ann B., et al. “Aerogels from Engineering Polymers: Polyimide and Polyamide Aerogels.” Springer Handbook of Aerogels, Springer, 2023, pp. 567–594.
[2] G. Churu, J. A. Demko, K. Kimminau, D. Lantz, H. McGuire, G. Van der Weil, M. Field, S. Malakooti, S. L. Vivod, “Thermal conductivity and mechanical properties of polymeric aerogels for cryogenic insulation applications,” IOP Conf. Series: Materials Science and Engineering 1302, 012007, 2024.
[3] G. Churu, J. A. Demko, A. Mole, R. C. Duckworth, H. Lu, S. Malakooti, and N. Leventis, “Thermal and Electrical Properties of Isocyanate Derived Organic Aerogels for Cryogenic Insulation Applications,” IOP Conf. Ser.: Mater. Sci. Eng. 756 012007, 2020.
[4] Fesmire, J.E., Johnson, W.L., Kelly, A.O., Meneghelli, B.J., and Swanger, A.S., "Flat Plate Boiloff Calorimeters for Testing of Thermal Insulation Systems," Advances in Cryogenic Engineering: Proceedings of the Cryogenic Engineering Conference (CEC) 2015, Vol. 101, Institute of Physics, 2016.
[5] J A Demko, J E Fesmire, W L Johnson, and A M Swanger, “Cryogenic Insulation Standard Data and Methodologies,” Advances in Cryogenic Engineering: Transactions of the Cryogenic Engineering Conference – CEC, American Institute of Physics, Vol. 59A, pp. 463-470, 2014.
[6] J A Demko, J E Fesmire, J Dookie, J Bickley, and S Kraft, “Comparison tests of cellular glass insulation for the development of cryogenic insulation standards,” Advances in Cryogenic Engineering: Proceedings of the Cryogenic Engineering Conference (CEC) 2015, Vol. 101, Institute of Physics, 2016.